Charring Ablators on Lifting Entry Vehicles

E. Arnold Reinikka* and Philip B. Wells†
The Boeing Company, Seattle, Wash.

Char-forming plastic materials are examined for capability of providing thermal protection of lifting vehicles (L/D = 0.5 to 1.5) entering the earth's atmosphere from near-earth orbits. A simplified theory for charring ablation materials is discussed. A rapid means is given for calculating aerodynamic heating encountered during lifting entry. Design charts based on these methods are shown for determining thermal protection weights when using microballooned phenolic nylon. These weights are based on maintaining a controlled environment for the cabin and load-carrying structures.

Nomenclature

c_p = specific heat, Btu/lb-°F
C_L = lift coefficient
C_D = drag coefficient
g = local acceleration of gravity, ft/sec²
H = heat-transfer coefficient based on enthalpy
H_P = heat of pyrolysis, Btu/lb
i = enthalpy, Btu/lb
k = thermal conductivity, Btu/ft-sec-°F
$\dot{m}$ = mass loss rate, lb/ft²-sec
$\dot{q}$ = heating rate, Btu/ft²-sec
R_e = radius of earth, ft
r = recovery factor
S = vehicle planform area, ft²
T_d = decomposition temperature, °F
T = temperature, °F
t = time, sec
V = velocity, fps
$\bar{V}$ = V/V_{sat}
W = vehicle weight, lb
x = distance, ft
Z = altitude, ft
Γ = mass fraction of solid converted to gas, $\dot{m}_g/\dot{m}_s$ const
ρ = density, lb/ft³
ψ = blocking function
γ = flight path angle, deg
θ = exponent involved in injection parameter (see Fig. 1)
ϵ = emissivity
σ = Stefan-Boltzmann constant, Btu/ft²-sec-°R
ϕ = bank angle, deg
δ = char thickness, ft
ξ = parameter defined in (5)

Subscripts

c = char layer
g = gas
a = air
rel = relative
I = inertial
i = initial
s = solid
sat = satellite
f = final
w = wall
r = recovery
∞ = freestream condition
0 = unblocked convective input
k = conducted into plastic

Presented as Preprint 63-181 at the AIAA Summer Meeting, Los Angeles, Calif., June 17–20, 1963; revision received October 31, 1963. The authors would like to express their appreciation to G. von Fuchs and R. Byington for performing the digital computations and to G. L. Dugger for his helpful editorial comments.

* Stress Analyst, Aero-Space Division.
† Research Engineer, Aero-Space Division. Member AIAA.

Introduction

VARIATIONS in entry missions, and in vehicle shapes and aerodynamic characteristics, have a strong effect on heat shield requirements. A rapid means for evaluating these requirements is desirable for preliminary design studies. A method employing an "effective heat of ablation" has been used for designing heat shields of noncharring ablators (Teflon, Avcoat "A," etc.), but analysis for char-forming ablation materials is more involved. The complete mathematical description of the conservation of energy and mass during the ablation process requires consideration of such factors as reaction kinetics, the transport of thermal radiation through the material, char removal by combustion and/or rupture due to thermal stresses, the thermal equilibrium (or lack of it) between the gases and the char, and the transient effects due to heat storage.[1–5] Lifting entry aggravates the thermal protection problem owing to the long times involved at moderately high heat fluxes. This creates a substantial requirement for insulation.

In the following text an approximate analysis for char-forming ablators is developed, and trajectory and aerodynamic heating calculations are then described. These calculations lead to the development of convenient normalized heating curves and to design charts for determining thermal protection requirements for ablation-cooled lifting vehicles using a char-forming plastic.

Ablation Analysis

In the approach taken here use is made of a relatively simple mathematical model. The material is divided into two regions; char layer and plastic, separated by the decomposition plane (see Fig. 1). The following assumptions are made:

1) All chemical reactions can be grouped into one single reaction that occurs at the decomposition plane, with one over-all heat of pyrolysis H_p. (Chemical reactions and radiation within the char layer are neglected.)

2) The temperature range over which the reactions occur can be approximated by a single, mean temperature T_d that remains constant.

With the foregoing assumptions, the energy equation in the char layer is

$$\rho_c c_c \frac{\partial T}{\partial t} + \dot{m} g c_{pg} \frac{\partial T}{\partial x} = \frac{\partial}{\partial x}\left(k_c \frac{\partial T}{\partial x}\right) \tag{1}$$

The boundary conditions at the decomposition plane ($X = 0$) are

$$T(0) = T_d = \text{const} \tag{2}$$

$$k_c(\partial T/\partial x)_{+0} = \dot{m}_s H_p + \dot{q}_{ks} \tag{3}$$

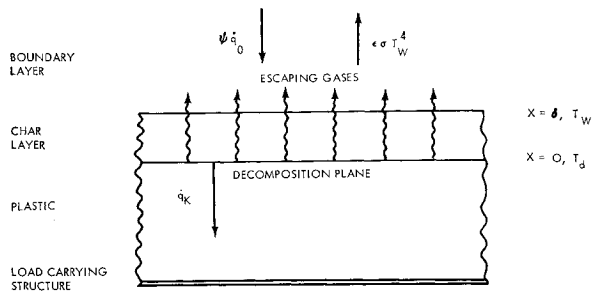

Fig. 1 Ablation process schematic.

where $\dot{q}_{ks} \equiv k_s(\partial T/\partial x)_{-0}$ ($\dot{q}_{ks}$ is the heat flux conducted into the plastic). It is calculated from the finite difference solution to the constant temperature-moving boundary, transient conduction problem in the plastic. Assuming quasi-steady state conditions, constant thermal properties, and constant $\Gamma = \dot{m}_g/\dot{m}_s$, Eq. (1) simplifies to

$$k_c(d^2T/dx^2) = \dot{m}_s\Gamma c_{pg}(dT/dx) \tag{4}$$

The general solution to (4) is

$$T(x) = c_1 + c_2e^{\xi x/\delta} \tag{5}$$

where $\xi = \dot{m}_s\Gamma c_{pg}\delta/k_c$. Applying boundary conditions (2) and (3) to (5) and rearranging yields

$$T_w = T_d + [H_p\xi/\Gamma c_{pg} + \dot{q}_{ks}\delta/k_c]F(\xi) \tag{6}$$

where

$$F(\xi) = \sum_{n=0}^{\infty} \frac{\xi^n}{(n+1)!} \tag{7}$$

From Eqs. (6) and (7), the limits are $\delta \to 0$, $T_w = T_d$ and $\dot{m}_s \to 0$, $T_w = T_d + \dot{q}\delta/k_c$.

For no char loss, the char thickness is given by

$$\delta = \frac{1-\Gamma}{\rho_c}\int_0^t \dot{m}_s dt \tag{8}$$

In order roughly to account for char removal, Eq. (8) is used until the char thickness reaches a specified value, after which it is held constant. For this study, the maximum char thickness was taken as 0.25 in.

A simple expression for mass loss rate of the plastic can now be formulated by considering the following energy balance for a control volume which enclosed the char layer:

$$\dot{m}_s = \frac{\psi\dot{q}_0 - \epsilon\sigma T_w^4 - \dot{q}_{ks}}{H_p + \Gamma c_{pg}(T_w - T_d)} \tag{9}$$

In Eq. (9), the reduction in convective heat transfer due to mass injection into the boundary layer is accounted for by the "blocking function" ψ defined as the ratio of convective heat flux with mass injection to that without mass injection under otherwise identical conditions. Thus, $\psi\dot{q}_0$ is the actual convective heat flux to the char surface during ablation. Studies indicate that for most cases of interest, the blocking function depends primarily on the parameter $(c_{pg}/c_{pa})^\theta\dot{m}_g(i_r - i_w)/\dot{q}_0$.

Figure 2 shows the curves used for the blocking function. For turbulent flow, the curve recommended by Bartle and Leadon[6] for supersonic, turbulent flow over a flat plate was used. The data of Ref. 7 were used for laminar flow plate.

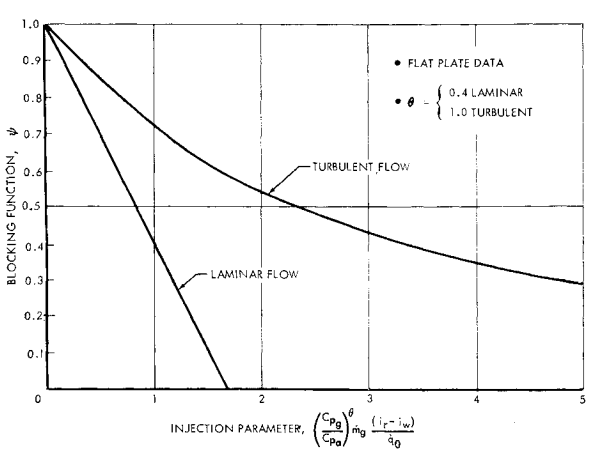

Fig. 2 Blocking functions used.

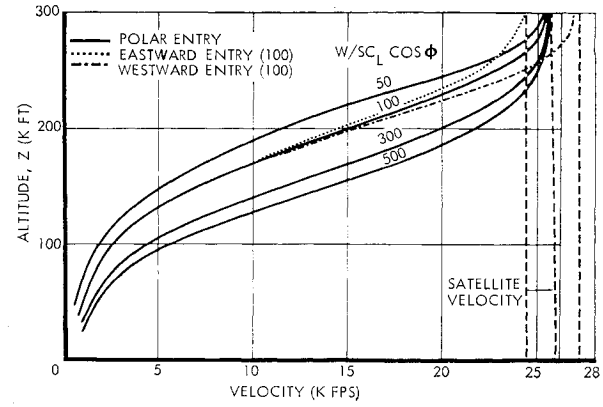

Fig. 3 Equilibrium glide paths.

Trajectories and Aerodynamic Heating

Lifting vehicles entering from near-earth orbits rapidly establish an equilibrium glide flight with a small flight path angle γ and a negligible rate of change of γ. Therefore it can be assumed that $d\gamma/dt \simeq 0$, $\sin\gamma \simeq 0$, and $\cos\gamma \simeq 1$, and that the radius of curvature of the flight path is equal to the radius of the earth. The equations describing such an equilibrium glide flight are

$$V_{rel}^2\cos\phi C_L S\rho_\infty/2 = W(1 - V_I^2)/gR_e \tag{10}$$

$$V_{rel}^2 C_D S\rho_\infty/2 = (W/g)dV/dt \tag{11}$$

It can be seen from (10) that $W/SC_L\cos\phi$ is the only vehicle characteristic required to define the altitude-velocity relationship of an equilibrium glide path. Solutions of (10) based on the 1959 ARDC atmosphere are presented in Fig. 3 for various values of $W/SC_L\cos\phi$ and various entry directions, respectively.

Substituting (10) into (11), solving for dt/dV, and integrating gives

$$\frac{t}{L/D} = \frac{R_e}{2(gR_e)^{1/2}}\ln\left[\left(\frac{1-\bar{V}_f}{1+\bar{V}_f}\right)\left(\frac{1+\bar{V}_i}{1-\bar{V}_i}\right)\right]\cos\phi \tag{12}$$

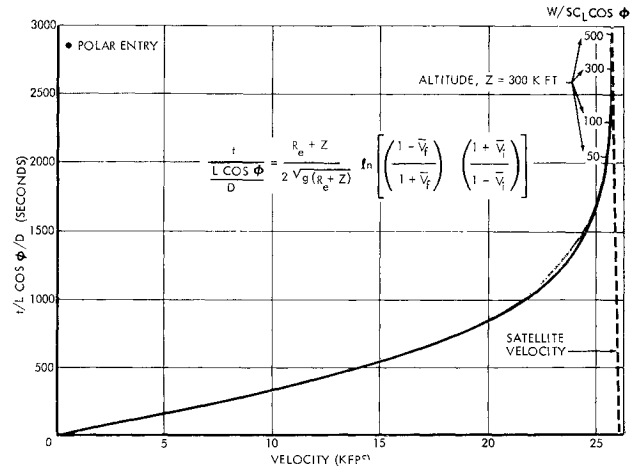

Fig. 4 Flight time along equilibrium glide paths.

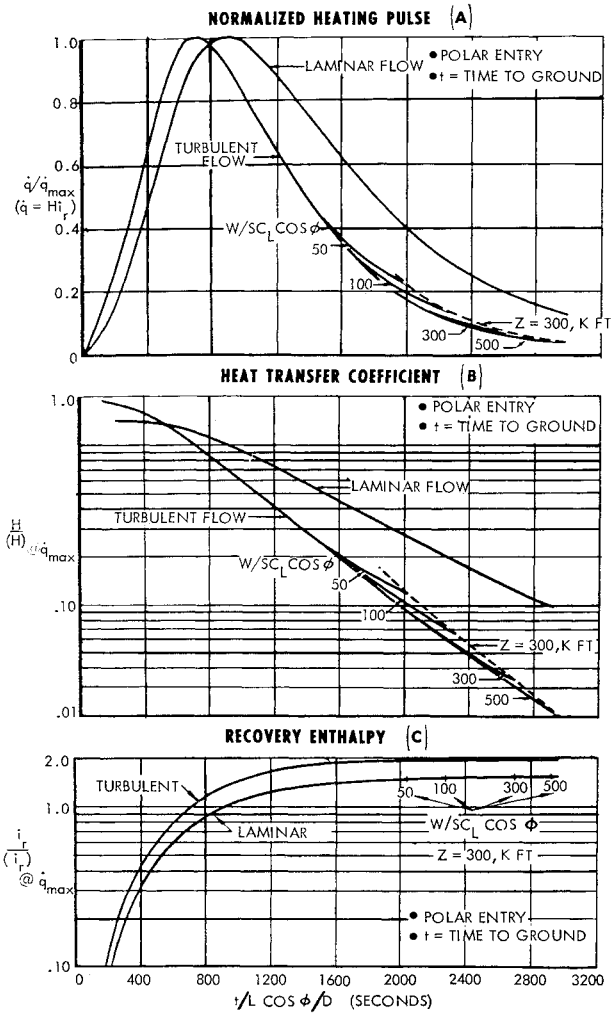

Fig. 5 Normalized heat-transfer parameters.

This equation is shown in Fig. 4. These equations and figures show that flight along equilibrium glide paths is uniquely expressed by defining the entry direction, $L\cos\phi/D$, and $W/SC_L\cos\phi$.

For lifting entry from orbital velocities, thermal radiation from the hot shock layer is negligible; therefore only convective heating is considered here. Furthermore, since boundary-layer recovery enthalpies i_r encountered on entry trajectories are much higher than the gas enthalpy at wall temperature, the heat-transfer coefficient H is essentially independent of wall temperature (and of wall material). Therefore it is convenient to deal with the cold wall heat flux $\dot{q} \equiv Hi_r$, as it is independent of the wall temperature and thus of the particular material being used.

For a particular vehicle configuration, attitude, location on a vehicle, and type of flow, this cold-wall heating rate is only a function of altitude and velocity. However, altitude-velocity profiles vary with $W/SC_L\cos\phi$. Moreover, the time-history of heating to a number of locations on a given vehicle (in a specific attitude) must be calculated to determine overall heat shield weights.

Heat-transfer coefficients were computed using Ref. 8 data, which were obtained by Eckert's reference temperature method[9, 10] in conjunction with heat-transfer formulas for incompressible flow over flat plates and wedges. The method of Fay and Riddell[11] was used for laminar flow at an axisymmetric stagnation point. From the results of these calculations it became apparent that the time-histories of H and i_r form families of similarly shaped curves for various $W/SC_L\cos\phi$. Thus, curves of $\dot{q} = Hi_r$ had similar shapes but different maximum values. It was found that plotting the ratio

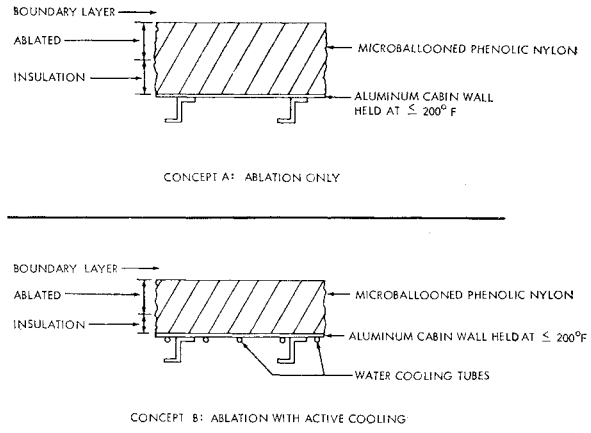

Fig. 6 Thermal protection concepts.

$\dot{q}/\dot{q}_{max}$ vs $t/(L/D)\cos\phi$ essentially produced one curve for laminar flow and another for turbulent flow (Fig. 5a). It was then possible to normalize the heat-transfer coefficient and recovery enthalpy to their values at the time when the cold-wall heat flux was a maximum. These are shown in Figs. 5b and c.

Figure 5b shows that for either laminar or turbulent flow, $H/H_{at\ \dot{q}\ max}$ is only a function of $t/(L/D)\cos\phi$, except for slight variations for the turbulent case at high altitudes.‡ The recovery enthalpy, $i_r = i_\infty + rV_\infty^2/2$, is primarily dependent on V_∞^2, which, for equilibrium glide, is only a function of $t/(L/D)\cos\phi$. Thus, it is not surprising that i_r is given by a single curve for either laminar or turbulent flow.

The normalized heating data of Fig. 5a are for polar entry, but there is very little effect of entry direction. The inertial velocity is given by $V_I = V_{rel} + 1550$ fps for eastward entry, whereas for westward, $V_I = V_{rel} - 1550$ fps. This difference creates $\pm 42/L/D$ sec in total entry time for equilibrium glide from 300,000 ft to the ground, which is insignificant for preliminary design purposes. Thus, the *normalized* heating curves are good approximations for any entry direction; the principle effect of variations in entry direction is that of changing the maximum value of the cold-wall heat flux, which is least for eastward entry and greatest for westward entry (Fig. 3).

Design Charts for Microballooned Phenolic Nylon

The normalized heating curves for turbulent flow in Fig. 5a provide a means for developing design charts for thermal protection requirements in lifting entry from near-earth orbits. The normalized heating curves were modified to include realistic landing maneuvers for the various L/D's, because for the ablation-only concept (Fig. 6) maximum backside temperatures occur toward the end of flight. This is due to the finite time required to dissipate heat stored in the ablation material. The thermal protection weights are based on keeping the cabin wall temperature $\leq 200°F$. Figure 6 shows the two thermal protection concepts that were evaluated. The boundary condition at the cabin wall is convective cooling for concept A, whereas for concept B it is constant tempera-

‡ It is not feasible to prove theoretically that this normalization exists because the equations required to relate the local flow conditions to the freestream conditions are complicated (flow across a shock wave), and the required data are available only in tabulated or graphical form. However, it seems reasonable that the heat-transfer coefficient should normalize, because it is proportional to certain parameters, such as the Reynolds number and Prandtl number, which depend on altitude and velocity, and altitude-velocity profiles are similarly shaped for various equilibrium glide paths.

Table 1 Properties of micro-ballooned phenolic nylon

Char		
ρ_c	Density, lb/ft^3	20
k_c	Conductivity, Btu/ft-°F-sec	8.9×10^{-5}
ϵ	Emissivity	0.85
Plastic		
ρ_s	Density, lb/ft^3	30
c_s	Specific heat, Btu/lb-°F	0.44
k_s	Conductivity, Btu/ft-°F-sec	1.8×10^{-5}
H_p	Heat of pyrolysis, Btu/lb	600
T_d	Temperature of decomposition, °F	1400
Γ	Mass fraction of solid converted to gas	0.73
Gas		
c_{pg}	Specific heat, Btu/lb, °F	0.78

ture. The properties of the ablation material are shown in Table 1.

It is recognized that the simplified ablation analysis only approximately accounts for char-layer removal (due to combustion and/or mechanical errosion) and the reaction kinetics of the virgin material decomposition. However, the following thermal protection design charts could be generated using a more sophisticated ablation analysis and/or different ablation materials. This procedure would affect the magnitude of the weights, but it would not affect the general method presented here.

Thermal protection weights per unit area and the major items that comprise these total weights are shown in Fig. 7 for the two heat-shield concepts. They are plotted as functions of cold wall $\dot{q}_{max}$ for lift/drag ratios of 0.5, 1.0, and 1.5. Safety factors of 1.25 for material ablated, 1.0 for plastic remaining for insulation, and 1.10 for water coolant have been incorporated in these curves.

Figure 7a shows that total entry time, which is proportional to $L\cos\phi/D$, has a considerably larger effect on total thermal protection weight than variations in $\dot{q}_{max}$. The amount of material ablated (for minimum total weight) is independent of the manner in which the cabin wall is cooled. Therefore, the comparison of concepts A and B involves a trade between the amount of ablation material remaining for insulation in concept A with the insulation weight plus water and cooling system weights in concept B. The water-cooling system weights in Figs. 7d and e, respectively, are based on use of a water-glycol solution which runs through a heat exchanger where heat is dissipated by water; the resulting steam is dumped overboard. The cooling system weight is independent of $L\cos\phi/D$, because its minimum weight occurs at approximately the same maximum heating rate into the water in all cases. The water weight is directly related to total heat input, which increases with decreasing heating rates, because the ablation mechanism becomes a less efficient means of dissipating heat as the heating rate decreases.

The thermal protection weights for ablation only (concept A) were determined by the method presented in Fig. 8. It was assumed that an internal environmental control system provided force convective cooling of the cabin wall with an average heat-transfer coefficient of 1 Btu/ft^{2}hr°F for a mean internal gas temperature of 70°F.

Thermal protection weights for concept B were optimized in the manner presented in Fig. 9. It is interesting to note that minimum weight occurs when the weight of ablation material remaining for insulation approximately equals the sum of water system and coolant weights.

The total (unblocked) input heating rate, $\dot{q}_0 = H(i_r - i_w)$, and the various ways this heat input is dissipated are presented in Fig. 10 as functions of entry time for turbulent flow with $L\cos\phi/D = 1.0$ and $\dot{q}_{max} = 50$ Btu/ft^2 sec. A very small percentage of the input heating actually goes into decomposing the ablation material. A significant portion, $(1 - \psi)\dot{q}_0$, is blocked by the injection of gases into the boundary layer. The difference between the remainder $\dot{q}_0$ and the reradiated heat flux, $\epsilon\sigma T_w^4$, is only 1 to 2 Btu/ft^2 sec, which is dissipated by the actual process of decomposition, heat conduction into the plastic, and heat absorbed by the gases passing through the char layer.

A comparison between weights for laminar and turbulent flow vs maximum char thickness for concept A is shown in Table 2. Maximum char thickness was varied due to the unknowns in the mechanisms of char-layer removal. Reference to Fig. 5 shows that, for a given maximum cold-wall heating rate and $L\cos\phi/D$, the total heat load (Btu/ft^2) is greater for laminar flow than for turbulent flow, whereas Fig. 2 shows that the blocking function is more efficient for laminar than turbulent flow. For the case of 0.25-in. maximum char

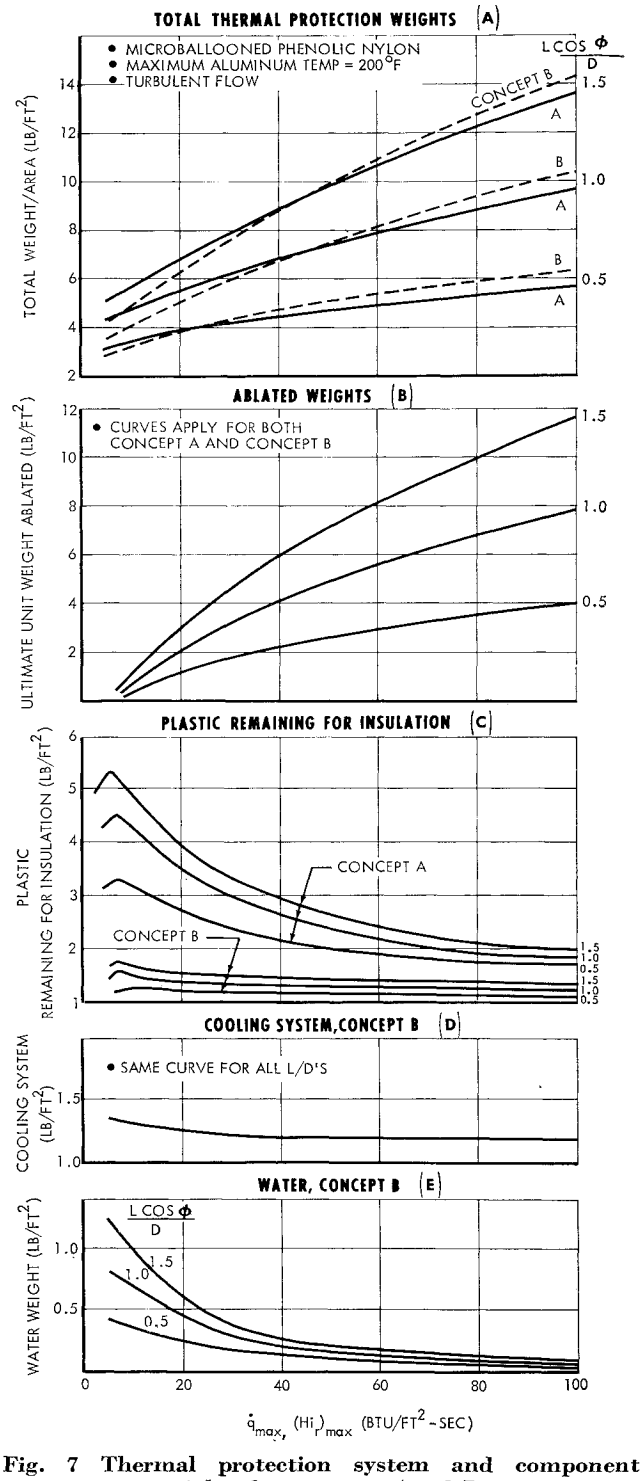

Fig. 7 Thermal protection system and component weights for concepts A and B.

thickness, these two effects tend to cancel one another, with the net effect that the weight for laminar flow is slightly greater. When no char is allowed to form ($\delta_{max} = 0$), the trend is reversed, because the mass loss rate for pure ablation is quite sensitive to the particular blocking function used (re-radiation from the 1400°F surface is relatively small). The case where $\delta_{max} = 0.10$ in. is between these two extremes, and the weights are nearly equal. It should be noted that for any particular location on a vehicle, the maximum cold-wall heating rate usually would be different for laminar or turbulent flow.

The normalized heating curves and design chart were used to determine the thermal protection requirements for two lifting entry vehicles X and Y with L/D's of 0.75 and 1.00, respectively (Table 3). Weights required to maintain 200°F cabin-wall temperature (ablation only, concept A) are given for flight at maximum hypersonic L/D (low vehicle attitude) and maximum lift coefficient C_L (high vehicle attitude). The weight ablated and weight remaining for insulation are shown; the latter predominates because there are large areas (upper surfaces) subjected to relatively low heating rates (on the order of 10 Btu/ft² sec or less) where very little ablation occurs. A large percentage of the aerodynamic heat is conducted into the plastic. This necessitates rather large thicknesses of plastic to maintain low backside temperatures.

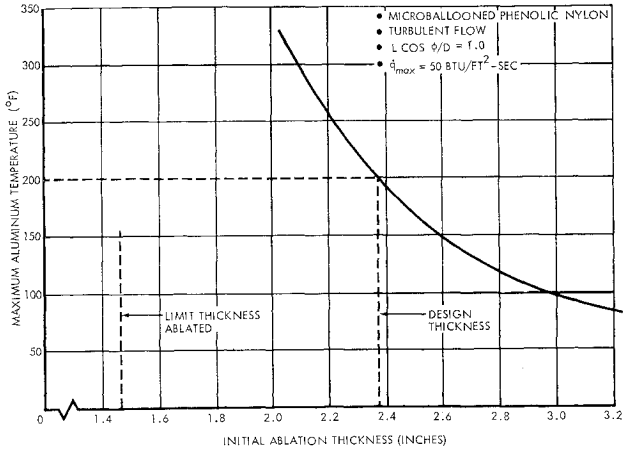

Fig. 8 Typical method of determining ablation requirements for concept *A*.

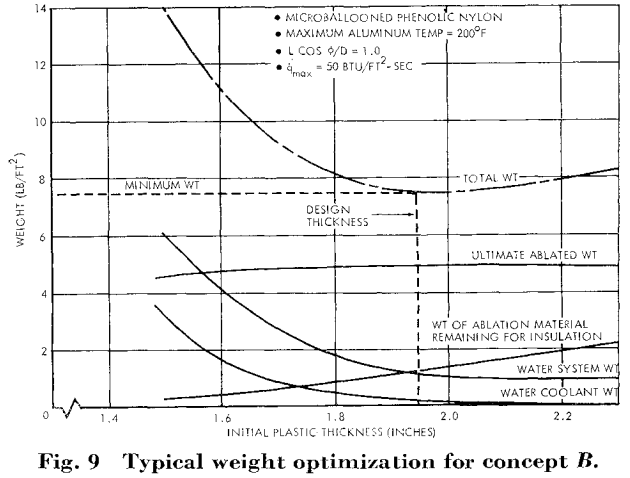

Fig. 9 Typical weight optimization for concept *B*.

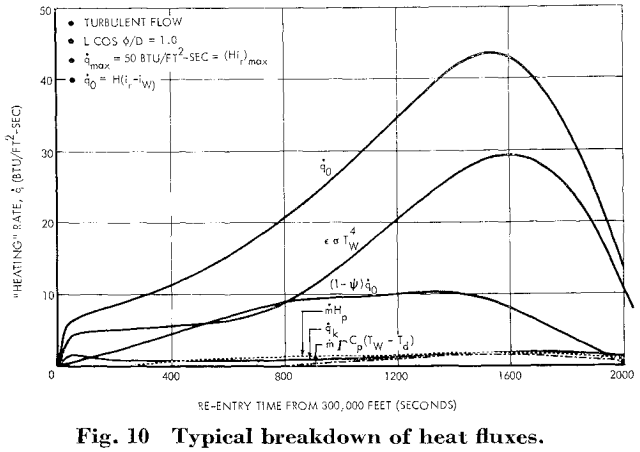

Fig. 10 Typical breakdown of heat fluxes.

Table 2 Effect of char-layer thickness and type of flow on thermal protection weight for concept *A* ($L/D \cos\phi = 1.0$; $\dot{q}_{max} = 50$ Btu/sec-ft²)

		Total weight/area, lb/ft²		
Flow type	Q_t, Btu/ft²	$\delta_{max} = 0$ in.	$\delta_{max} = 0.10$ in.	$\delta_{max} = 0.25$ in.
Laminar	60,500	14.3	11.1	8.2
Turbulent	51,000	17.0	10.5	7.3

Table 3 Effect of vehicle L/D and attitude on thermal protection weight for concept *A*—polar entry; turbulent flow

			Plastic weight, lb		
Vehicle	Attitude	$(L/D)\cos\phi$	Ablated	Insulation	Total
X	CL_{max}	0.60	170	1080	1250
	$(L/D)_{max}$	0.75	480	1240	720
Y	CL_{max}	0.51	220	680	900
	$(L/D)_{max}$	1.00	800	970	1770

Conclusions

1) A convenient method for presenting normalized convective heat-transfer parameters for lifting entry from near-earth orbits was found.

2) Design charts for estimating weights of two types of thermal protection systems involving char-forming ablators were developed. These charts were based on a simplified ablation theory and estimated material properties for microballooned phenolic nylon. The same techniques could be applied with other materials and/or a more refined ablation analysis.

3) The difference in total thermal protection system weights without (A) and with (B) water cooling was small; A was slightly better for $\dot{q}_{max} = 20$, and B was slightly better for $\dot{q}_{max} = 40$ Btu/ft² sec.

References

[1] Scala, S. M. and Gilbert, L. M., "Thermal degradation of char-forming plastics during hypersonic flight," ARS J. **32**, 917–924 (1962).

[2] Swann, R. T. and Pittman, C. M., "Numerical analysis of the transient response of advanced thermal protection systems for atmospheric re-entry," NASA TN D-1370 (1962).

[3] Munson, T. R. and Spindler, R. J., "Transient thermal behavior of decomposing materials, Part 1: General theory and application to convective heating," IAS Preprint 62-30 (January 1962).

[4] Lafazan, S. and Siegel, B., "Ablative thrust chambers for space application," Am. Inst. Chem. Engrs. Preprint 5 (February 1962).

[5] McFarland, B., Joerg, P., and Taft, M., "Criteria for plastic ablation materials as functions of environmental parameters: Part 1, Results of analytical studies," Tech. Doc. Rept. Acronaut. Syst. Div. TR-61-439 (May 1962).

[6] Bartle, E. R. and Leadon, B. M., "The effectiveness as a universal measure of mass transfer cooling for a turbulent boundary layer," 1962 Heat Transfer and Fluid Mechanics Institute

(Stanford University Press, Stanford, Calif., 1962).

[7] Sziklas, E. A. and Banas, O. M., "Mass transfer cooling in compressible laminar flow," D. J. Masson (Comp.), "Mass transfer cooling for hypersonic flight," The Rand Corp., Paper S-51 (June 24, 1957).

[8] *Aerodynamic Heat Transfer Handbook* (Boeing Aircraft Co., Seattle, Wash., May 1961) Doc. D2-9514, Vol. 1.

[9] Eckert, E. R. B., "Survey on heat transfer at high speeds," Wright Air. Dev. Center. TR 54-70 (April 1954).

[10] Eckert, E. R. G., "Survey of boundary layer heat transfer at high velocities and high temperatures," Wright Air Dev. Center TR 59-624 (April 1960).

[11] Fay, J. A., and Riddell, F. R., "Theory of stagnation point heat transfer," J. Aeronaut. Sci. **25**, 73 (1958).

JANUARY 1964 J. SPACECRAFT VOL. 1, NO. 1

Range Maximization of a Surface-to-Surface Missile with In-Flight Inequality Constraints

WALTER F. DENHAM*
Raytheon Company, Bedford, Mass.

The use of aerodynamic lift during (planar) re-entry is considered in maximizing the range of a surface-to-surface missile. The attitude history (which also gives thrust direction) from launch through re-entry is optimized by the steepest-ascent procedure to maximize the surface range at impact. Two inequality constraints are included: 1) a limit on the pitch rate during boost; and 2) a limit on the normal load during re-entry. The results show that a substantially different maximum-range trajectory is obtained with modulated lift rather than with purely ballistic re-entry. The range increase for a 2300-naut-mile ballistic missile is significant if the normal load limit is over 5 *g*'s.

Introduction

THE optimization of rocket vehicle trajectories has been and continues to be of active interest. One major division considers the (vertically launched) surface-to-surface missile. Probably the most common measure of performance is the range capability with a given payload or, conversely, the payload achievable for a specified range. For ballistic re-entry vehicles this problem is one of ascent trajectory optimization. Over a two-dimensional nonrotating spherical earth, the trajectory is entirely determined from the vehicle's (pitch) attitude history during boost. This case has received ample investigation. Generally speaking, the optimal ascent consists of an initial pitch-over period followed by an essentially gravity turn. The particular optimization depends largely on the model assumed for the pitch-over. The use of aerodynamic lift during re-entry offers two advantages: range can be increased, and some measure of interceptor evasion may be gained through maneuvering. We shall consider only the range maximization problem.

We include two inequality constraints that are felt to be particularly relevant to this problem. The first is that the pitch-rate during boost is limited to a maximum value. The missile flies vertically for a prescribed interval and then begins pitching down. We anticipate that the initial pitch-rate will be the maximum value, but this is not demanded. The second constraint is a limitation on the normal force that may be permitted during re-entry. In this investigation the vehicle at re-entry is the same as it is at booster burnout. A vehicle that was designed to have additional lifting surfaces during re-entry could withstand greater normal loads and thus could achieve a greater range increase.

Received July 8, 1963; revision received October 9, 1963. This paper is adapted from the author's Dissertation for Harvard University. The work was wholly sponsored by Raytheon Company.

* Now Research Fellow, Division of Engineering and Applied Physics, Harvard University, Cambridge, Mass.

In this two-dimensional analysis the lift is determined by the vehicle's attitude (and, of course, the dynamic pressure). Hence, the entire trajectory is determined by the attitude, or the equivalent angle of attack which we shall actually use for convenience, program. The angle of attack gives thrust direction and aerodynamic forces during boost and the aerodynamic forces during the glide. Our goal is to obtain the angle-of-attack history (the control program) which maximizes the impact range while satisfying the inequality constraint relations.

For this problem the necessary conditions for the desired optimal solution are readily available, going back as far as Valentine in 1937.[6] Until recent years, however, these would have been only of academic interest. The currently available digital computers make iterative solution of many variational problems now within reach. Although more than one method has been used successfully in certain problems, the steepest-ascent (or gradient) method has been most useful to date in atmospheric trajectory optimization. This scheme, originated independently by H. J. Kelley and by A. E. Bryson Jr., has become a well-known optimization tool. Relatively little has been published thus far with inequality constraints, and a major purpose of this paper is to present an interesting problem including them.

In the steepest-ascent technique as described in Refs. 1–3, each successive improvement is the greatest attainable for a selected value of the integral of the control variable change squared multiplied by a time variable weighting function.† The weighting function, which to a large extent determines the efficiency of the iteration procedure, has yet received little attention. In this problem the sensitivity to angle-of-attack changes is many times greater in booster than in re-entry. The steepest-ascent method without the weighting function would have poor convergence properties for the re-entry angle-of-attack program. The weighting function is used to

† The integral involves a quadratic form in all of the control variable changes if there is more than one.